J|A|C|S
ARTICLES
Published on Web 06/18/2005

Conformational Constraint as a Means for Understanding RNA-Aminoglycoside Specificity

Kenneth F. Blount,[†,§] Fang Zhao,[†] Thomas Hermann,[‡] and Yitzhak Tor*[,†]

Contribution from the Department of Chemistry and Biochemistry, University of California, San Diego, La Jolla, California 92093-0358 and Anadys Pharmaceuticals, Inc., 3115 Merryfield Row, San Diego, California 92121

Received February 12, 2005; E-mail: ytor@chem.ucsd.edu

Abstract: The lack of high RNA target selectivity displayed by aminoglycoside antibiotics results from both their electrostatically driven binding mode and their conformational adaptability. The inherent flexibility around their glycosidic bonds allows them to easily assume a variety of conformations, permitting them to structurally adapt to diverse RNA targets. This structural promiscuity results in the formation of aminoglycoside complexes with diverse RNA targets in which the antibiotics assume distinct conformations. Such differences suggest that covalently linking individual rings in an aminoglycoside could reduce its available conformations, thereby altering target selectivity. To explore this possibility, conformationally constrained neomycin and paromomycin analogues designed to mimic the A-site bound aminoglycoside structure have been synthesized and their affinities to the TAR and A-site, two therapeutically relevant RNA targets, have been evaluated. As per design, this constraint has minimal deleterious effect on binding to the A-site. Surprisingly, however, preorganizing these neomycin-class antibiotics into a TAR-disfavored structure has no deleterious effect on binding to this HIV-1 RNA sequence. We rationalize these observations by suggesting that the A-site and HIV TAR possess inherently different selectivities toward aminoglycosides. The inherent plasticity of the TAR RNA, coupled to the remaining flexibility within the conformationally constrained analogues, makes this RNA site an accommodating target for such polycationic ligands. In contrast, the deeply encapsulating A-site is a more discriminating RNA target. These observations suggest that future design of novel target selective RNA-based therapeutics will have to consider the inherent "structural" selectivity of the RNA target and not only the selectivity patterns displayed by the low molecular weight ligands.

Introduction

In the mandated search for new approaches to target pathogens, viral and bacterial RNA sequences have recently emerged as intriguing targets.[1,2] Key events in bacterial and viral life cycles that are mediated by RNA or RNA−protein interactions present vulnerable points at which RNA-binding small molecules could capitalize.[3−5] Observations linking the interference of protein synthesis by aminoglycosides with their direct binding to the ribosomal decoding site (A-site) were the first example of this RNA targeted approach.[6,7] Recently, the aminoglycosides have been the focus of more intense study, with the observation that they can inhibit the activity of several ribozymes[8] or can bind to two important HIV-1 RNAs, the RRE and the TAR, thereby preventing the necessary binding of their cognate protein.[9]

The ability of aminoglycosides to bind diverse RNA targets has an unfortunate caveat: these antibiotics are rather promiscuous RNA binders. This promiscuity is partly a result of their electrostatically driven RNA binding mode.[10] From an electrostatic viewpoint, it is likely to be difficult to distinguish different RNA folds in solution. This problem is exacerbated by the ability of the aminoglycosides to conformationally adapt to diverse RNA targets. For example, neomycin B, **1a**, or the closely related paromomycin, **1b**, (Figure 1a) assumes a different conformation, when bound to different RNA targets[11−14] (Figure

[†] University of California.
[‡] Anadys Pharmaceuticals.
[§] Current address: Molecular, Cellular, and Developmental Biology, Yale University, 266 Whitney Avenue, KBT 516, New Haven, Connecticut 06520.

(1) Tor, Y. *Angew. Chem., Int. Ed.* **1999**, *38*, 1579−1582.
(2) For selected review articles, see: Hermann, T.; Westhof, E. *Curr. Opin. Biotechnol.* **1998**, *9*, 66−73. Ritter, T. K.; Wong, C.-H. *Angew. Chem., Int. Ed.* **2001**, *40*, 3508−3533. Griffey, R. H.; Swayze, E. C. *Expert Opin. Ther. Pat.* **2002**, *12*, 1367−1374.
(3) Tor, Y. *ChemBioChem* **2003**, *4*, 998−1007.
(4) For selected review articles, see: Chow, C. S.; Bogdan, F. M. *Chem. Rev.* **1997**, *97*, 1489−1513. Michael, K.; Tor, Y. *Chem.—Eur. J.* **1998**, *4*, 2091−2098. Afshar, M.; Prescott, C. D.; Varani, G. *Curr. Opin. Biotechnol.* **1999**, *10*, 59−63. Wilson, W. D.; Li, K. *Curr. Med. Chem.* **2000**, *7*, 73−98. Sucheck, S. J.; Wong, C.-H. *Curr. Opin. Chem. Biol.* **2000**, *4*, 678−686.
(5) Hermann, T. *Angew. Chem., Int. Ed.* **2000**, *39*, 1891−1905.
(6) Schroeder, R.; Waldsich, C.; Wank, H. *EMBO J.* **2000**, *19*, 1−9.
(7) Von Ahsen, U.; Noller, H. F. *Science* **1993**, *260*, 1500−1503.
(8) Stage, T. K.; Hertel, K. J.; Uhlenbeck, O. C. *RNA* **1995**, *1*, 95−101. Wang, H.; Tor, Y. *J. Am. Chem. Soc.* **1997**, *119*, 8734−8735.
(9) Zapp, M. L.; Stern, S.; Green, M. R. *Cell* **1993**, *74*, 969−978. Mei, H. Y.; Mack, D. P.; Galan, A. A.; Halim, N. S.; Heldsinger, A.; Loo, J. A.; Moreland, D. W.; Sannes-Lowery, K. A.; Sharmeen, L.; Truong, H. N.; Czarnik, A. W. *Bioorg. Med. Chem.* **1997**, *5*, 1173−1184.
(10) Tor, Y.; Hermann, T.; Westhof, E. *Chem. Biol.* **1998**, *5*, R277−283.
(11) Fourmy, D.; Recht, M. I.; Blanchard, S. C.; Puglisi, J. D. *Science* **1996**, *274*, 1367−1371.
(12) Faber, C.; Sticht, H.; Schweimer, K.; Rosch, P. *J. Biol. Chem.* **2000**, *275*, 20660−20666.
(13) Jiang, L.; Majumdar, W. H.; Jaishree, T. J.; Weijun, X.; Patel, D. J. *Structure* **1999**, *7*, 817−827. Varani, L.; Spillantini, M. G.; Goedert, M.; Varani, G. *Nucleic Acids Res.* **2000**, *28*, 710−719.
(14) Vicens, Q.; Westhof, E. *Structure* **2001**, *9*, 647−658.

10.1021/ja050918w CCC: $30.25

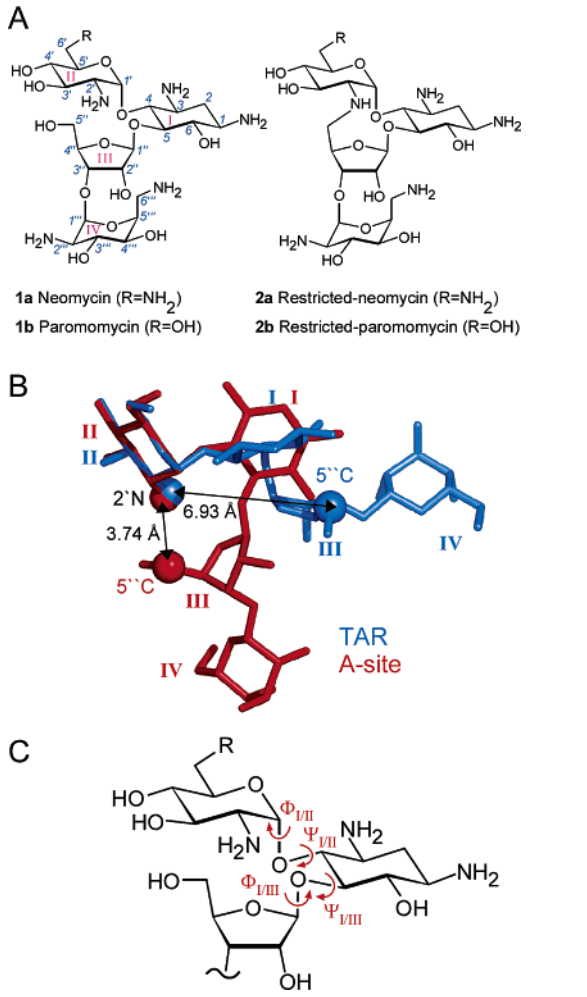

Figure 1. (A) Chemical structures of the neomycin class aminoglycosides studied. Neomycin B (**1a**) and paromomycin (**1b**) differ only at the 6′ position. Likewise, restricted neomycin (**2a**) and restricted paromomycin (**2b**) differ only at this position. Ring numbers are shown in red roman numerals. (B) The structure of neomycin bound to the TAR (blue) is overlaid with the structure of paromomycin bound to the A-site (red). The two structures were overlaid using the Pymol Molecular Graphics System based on a best fit of ring II. The 2′N-to-5″-C distances are indicated. (C) Torsional angles for the glycosidic linkages defined as $\Phi_{I/II}$ (O1′−C1′−O4−C4), $\Psi_{I/II}$ (C1′−O4−C4−C3), $\Phi_{I/III}$ (C5−O5−C1″−O1″), and $\Psi_{I/III}$ (C4−C5−O5−C1″).

1b). When bound to the prokaryotic ribosomal A-site,[14] the aminoglycoside is compactly arranged, with rings II and III in spatial proximity. In contrast, when bound to the HIV-1 TAR,[12] the aminoglycoside is in a more extended conformation, with rings II and III distal to one another. The aminoglycoside conformation is still different when bound to other RNA targets (see Supporting Information, Figure S.16). Although the relative positions of the individual neomycin rings differ among the complexes, the affinity with which neomycin or paromomycin binds each target is not dramatically different.

In an attempt to circumvent this conformational flexibility and the resulting RNA target promiscuity, conformationally constrained aminoglycoside analogues have been designed, synthesized, and evaluated.[15−17] Covalently "freezing" the aminoglycoside conformation may, under ideal circumstances, yield the following advantageous features: (a) increased affinity to the desired target due to limited entropy losses upon binding and (b) increased selectivity by locking the aminoglycoside skeleton in an unfavorable orientation for binding to competing targets. In this contribution we describe the design and synthesis of two new restricted aminoglycoside analogues **2a** and **2b** (Figure 1a), which are specifically designed to exhibit enhanced selectivity for the A-site relative to the TAR. A comparison of the RNA binding affinities of these novel products and their parent, nonrestricted counterparts suggests that conformationally restricted aminoglycosides show promise as target-selective binders, but the A-site and TAR RNAs may exhibit a different level of structural selectivity.

Results

Design of Conformationally Restricted Aminoglycosides. Antibiotics of the neomycin class exhibit very different structural features when bound to either the A-site RNA or the HIV-1 TAR (Figure 1b). All three published structures of paromomycin bound to the A-site reveal a similar structure, with a very compact arrangement of the four rings and rings II and III in spatial proximity.[11,15,18] Additionally, the B-factors reported for these structures indicate that the bound conformations of rings I and II are fairly static, while rings III and IV are increasingly dynamic. In contrast, when bound to the TAR, the antibiotics are more dynamic and assume a more extended conformation.[12] The published structure of TAR-bound neomycin includes a collection of 17 refined NMR structures and reveals two primary conformations, with a range of glycosidic torsion angles among the first three rings (Figure 1c; Table 1). In both conformations, rings II and III are distal to one another. Notably, the torsional angles between rings I and III in both TAR-bound conformations are very different from the torsional angles in any of the A-site bound paromomycin structures.

Given these major structural differences, we reasoned that a short covalent link between rings II and III should constrain the aminoglycoside into a structure resembling the A-site bound form, thereby altering its RNA affinity and target selectivity. The 2′-nitrogen and 5″-carbon were chosen for placement of the linker, identifying compounds **2a** and **2b** as our target molecules (Figure 1b). The average distance between these two atoms is 3.67 Å when bound to the A-site,[14] whereas the average distance between these two atoms in the TAR-neomycin structures is 6.9 ± 0.6 Å (standard deviation), further underscoring the significant conformational difference between the two interactions. Since the newly formed covalent bond would span a length of approximately 1.5 Å, these restricted aminoglycosides were expected to bind more readily to the A-site than to the TAR.

To predict the conformational effect induced by the covalent linker, we performed molecular dynamics simulations of **1a** and **2a** in water. Using the AMBER molecular dynamics simulation program, 100 iterative rounds were performed of phases of heating to 5000 K followed by cooling. Following energy

(15) For other approaches for exploring and improving aminoglycosides' RNA specificity, see: Alper, P. B.; Hendrix, M.; Sears, P. S.; Wong, C.-H. *J. Am. Chem. Soc.* **1998**, *120*, 1965−1978. Wong, C. H.; Hendrix, M.; Priestley, E. S.; Greenberg, W. A. *Chem. Biol.* **1998**, *5*, 397−406.
(16) Luedtke, N. W.; Liu, Q.; Tor, Y. *Biochemistry* **2003**, *42*, 11391−11403.
(17) A related approach has been explored for controlling oligosaccharide interactions. See: Bundle, D. R.; Alibes, R.; Nilar, S.; Otter, A.; Warwas, M.; Zhang, P. *J. Am. Chem. Soc.* **1998**, *120*, 5317−5318. Bundle, D. R.; Alibes, R.; Nilar, S.; Otter, A.; Warwas, M.; Zhang, P. *J. Am. Chem. Soc.* **1998**, *120*, 5317−5318. Navarre, N.; Amiot, N.; van Oijen, A.; Imberty, A.; Poveda, A.; Jiminez-Barbero, J.; Cooper, A.; Nutley, M. A.; Boons, G. *Chem.—Eur. J.* **1999**, *5*, 2281−2294. Wacowich-Sgarbi, S. A.; Bundle, D. R. *J. Org. Chem.* **1999**, *64*, 9080−9089.
(18) Carter, A. P.; Clemons, W. M.; Brodersen, D. E.; Morgan-Warren, R. J.; Wimberly, B. T.; Ramakrishnan, V. *Nature* **2000**, *407*, 897−902.

Table 1. Conformational Properties of RNA Bound Aminoglycosides

	$\Phi_{I/II}$[a]	$\Psi_{I/II}$	$\Phi_{I/III}$	$\Psi_{I/III}$	2′N/5″C distance (Å)	reference
paromomycin-A-site NMR	78.1	−145.0	−118.1	116.2	4.38	11
paromomycin-A-site crystal[b]	80.6	−150.9	−90.5	160.2	3.67	14
neo-TAR Class 1[c]	111.6	−42.0	−23.0	−51.7	7.24	12
neo-TAR Class 2	89.2	−94.1	−175.5	129.8	6.36	12

[a] $\Phi_{I/II}$ (O1′−C1′−O4−C4), $\Psi_{I/II}$ (C1′−O4−C4−C3), $\Phi_{I/III}$ (C5−O5−C1″−O1″), $\Psi_{I/III}$ (C4−C5−O5−C1″). [b] Numbers are an average of two bound paromomycin molecules in an asymmetric unit. [c] Torsional angles for TAR-bound neomycin are averages of 11 structures (class 1) or 6 structures (class 2) of the collected set of 17 best-fit structures.

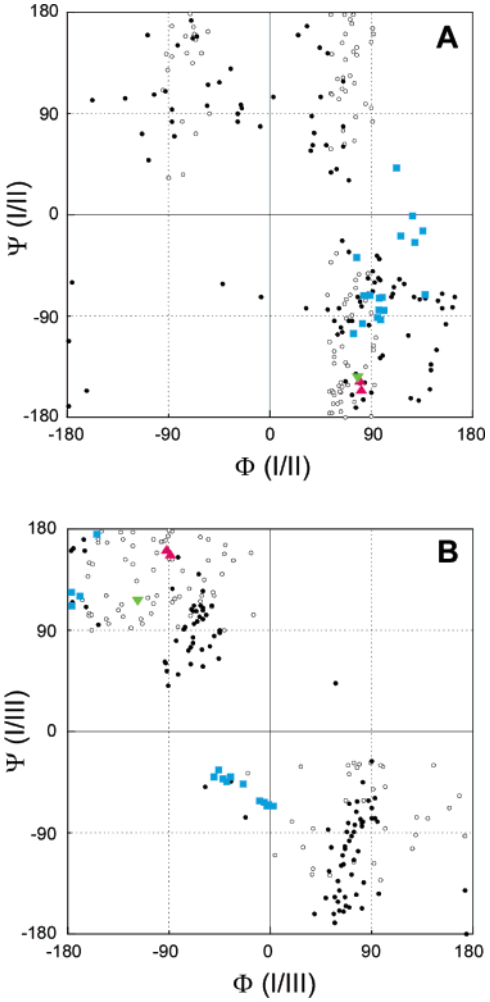

Figure 2. Torsional angles of aminoglycosides free in solution or bound to A-site or the TAR RNAs. (A) Torsional angles encountered during molecular dynamics simulations in water are shown for neomycin **1a** (open circles) and restricted neomycin **2a** (closed circles). Note the tighter distribution of **2a** conformations. Torsional angles of TAR-bound neomycin are shown in blue. Torsional angles of paromomycin **1b** when bound to the A-site as determined by NMR[11] or crystallography[14] are shown in green or red, respectively.

minimization, the torsional angles between each of the first three rings of the cooled conformation were recorded, and their distributions were examined (Figure 2). Interestingly, the conformational space available to the restricted **2a** is very similar to that available to **1a**. The primary difference is that the distribution of different conformations is somewhat more scattered for the nonrestricted **1a**, particularly around the glycosidic bond connecting rings I and III (Figure 2b). This difference is consistent with the expected reduction of conformational flexibility enforced by the covalent linkage. Importantly, the torsional angles in the A-site-bound paromomycin structures (triangles) are very similar to those predicted in this simulation for neomycin and restricted neomycin (open and filled circles, respectively). The slight differences that are observed likely represent minor structural adaptations that occur upon RNA binding.

It is informative to locate the TAR-bound neomycin conformation within this map. The published structure of TAR-bound neomycin includes a collection of 17 refined models which best fit the observed NMR data.[12] The range of torsional angles between rings I and III within these models (blue, Figure 2) represents a conformational family that is distinctive from that encountered in the solvent simulation for either **1a** or **2a**. Consistent with our design concept, this predicts that it would be energetically disfavored for the restricted **2a** to assume a conformation necessary for binding to the TAR. Thus, both the conformations obtained from the molecular dynamics simulations and the 2′N/5″C distance constraint imposed by the linker predict that **2a** and **2b** should bind less well than the parent **1a** and **1b** to the TAR, thereby altering target selectivity.

Synthesis. A concise synthesis of the restricted aminoglycoside analogues has been developed (Scheme 1). A fully Boc-protected neomycin was activated at the 5″ position with 2,4,6-triisopropylbenzenesulfonyl chloride to give **3** as previously reported[19] (Scheme 1a). TFA-mediated deprotection of all Boc groups, followed by dilution and neutralization with Et_3N, facilitated a slow (10 days) intramolecular cyclization to give the desired **2a**. To simplify isolation, this highly polar product was first protected as the penta-Boc derivative **4** and column purified. Acidic deprotection of all Boc groups followed by reversed-phase purification afforded **2a** in 12% overall yield (based on **3**).[20]

The conformationally restrained paromomycin derivative **2b** was prepared in a fashion similar to **2a** (Scheme 1b). To ensure 5″-selective activation of paromomycin **1b** that contains two primary alcohols, the 6′-hydroxyl was first protected as the isopropylidene ketal. Boc protection of all amines and activation of the 5″ position proceeded smoothly to yield **5**. The ketal group was then conveniently removed under the same conditions utilized for Boc deprotection, providing the 5″-activated paromomycin (Scheme 1b). After neutralization and high dilution cyclization, followed by a similar protection/purification/deprotection scheme, the conformationally restrained paromomycin **2b** was obtained in 20% overall yield (based on **5**).

It is important to note that protection of both conformationally constrained analogues **2a** and **2b** has always yielded (n − 1) protected derivatives **4** and **6**, respectively (where n is the total number of amines), as confirmed by NMR and MS analysis.[21]

(19) Michael, K.; Wang, H.; Tor, Y. *Bioorg. Med. Chem.* **1999**, *7*, 1361−1371.
(20) See Supporting Information for synthetic procedures and characterization.
(21) The NH peaks are well-resolved in acetone/d_6-DMSO/d_6 (3:1) and full assignment shows that the 2′-N is lacking a Boc group.

Scheme 1. Synthesis of Conformationally Constrained Analogues **2a** and **2b**[a]

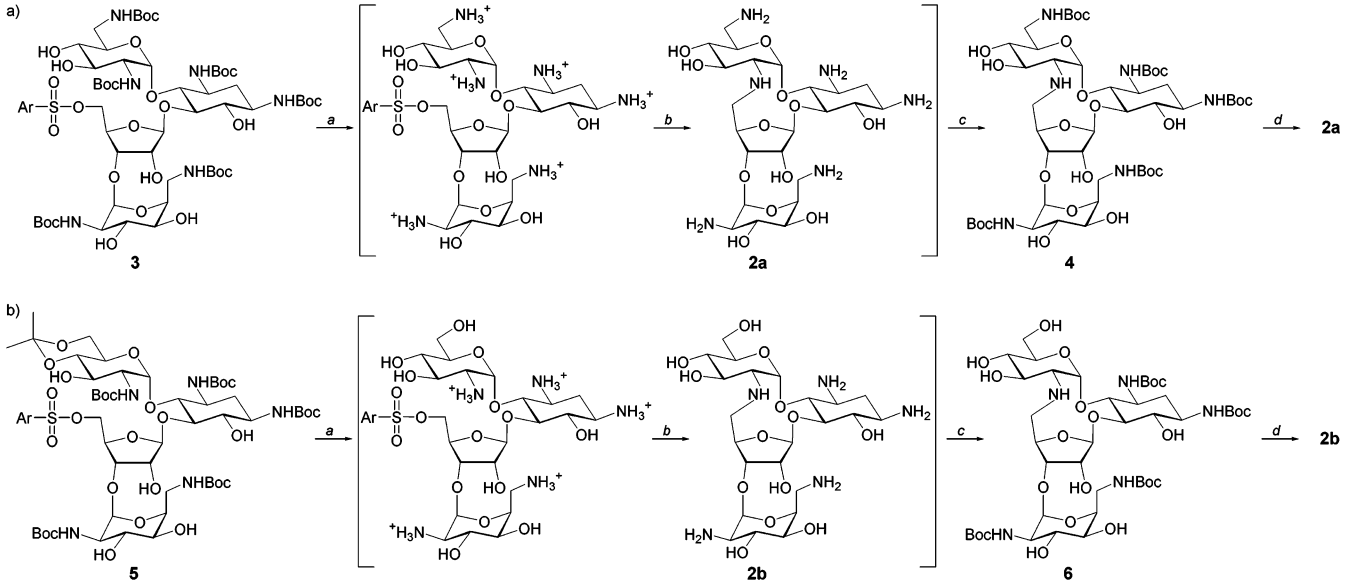

[a] Reagents and conditions: (a) TFA, $CHCl_3$; (b) NEt_3, DMF; (c) Boc_2O, NEt_3, methanol; (d) TFA, $CHCl_3$. Ar = 2,4,6-triisopropylbenezene.

In both cases the least reactive amine is the newly formed bridging secondary amine. This lower nucleophilicity may be a result of steric or electronic effects. These reactivity observations are pertinent to the RNA binding characteristics of the new derivatives as elaborated below.

Spectroscopic Characterization. The intramolecular cyclization imposes a significant conformational constraint on the aminoglycosidic skeleton. In terms of composition, however, the cyclized structures **2a** and **2b** can essentially be viewed as "dehydrated" antibiotics (i.e., the two structures differ only by a molecule of water). To unequivocally prove the formation of the N−C bond between the amine at the 2′ position and the 5″ carbon on the D-ribose, a series of NMR experiments has been conducted to assign all resonances and establish the cyclization site.

A qualitative comparison of the ^{1}H NMR spectra of the restricted neomycin derivative **2a** and its parent natural product **1a** reveals intriguing and informative changes.[22] The ^{1}H NMR spectrum of the cyclized derivative, under the same pH and counteranion conditions, shows a dramatic upfield shift of the 5″ methylene group, when compared to neomycin's spectrum.[22] This observation is in full agreement with the replacement of an oxygen by a nitrogen functional group replacement. The change in chemical shift pulls the 5″-H_b peak out of a crowded spectral region and significantly facilitates its assignment. Interestingly, the rest of the proton signals of the D-ribose system (ring III) experience a dramatic downfield shift.[22] The anomeric proton ($H_{1''}$) shifts further downfield to $H_{1'}$, a rare observation for neomycin derivatives. These extraordinary changes in chemical shifts are likely due to a significant conformational distortion of the D-ribose ring enforced by the intramolecular cyclization.

The full assignment of compound **2a** was accomplished using 1D proton NMR as well as 2D gradient-assisted correlation spectroscopy (gCOSY), gradient-assisted heteronuclear single quantum coherence (^{1}H−^{13}C gHSQC) and heteronuclear multiple bond correlation (^{1}H−^{13}C gHMBC) spectroscopies. The anomeric protons of rings II, III, IV (δ 5.0−6.0) and the methylene protons of ring I (δ = 2.58 and 1.94) provide a convenient starting point, and gCOSY spectra assist in assigning the proton system of each ring (see Supporting Information for all spectra). Phase sensitive gHSQC spectra provide a definitive assignment for all methylene groups at positions 2, 6′, 5″ and 6‴ (see Figure 1 for numbering). Edited gHSQC spectra differentiate the carbons connected to oxygen (δ > 55.0) from the carbon centers connected to nitrogen or other carbon atoms (δ < 55.0), with one exception: 2′-C at 60.2 ppm.[23,24] This significant downfield shift is consistent with converting the primary amine at this position to a secondary amine.[23] Full assignment was not possible until ^{1}H−^{13}C gHMBC spectroscopy unequivocally secured the assignment of ring II and ring IV by showing correlations across the glycosidic bonds (i.e., 4-H to 1′-C, 4-C to 1′-H, 3″-H to 1‴-C, 3″-C and 1‴-H).[25] It is important to note that this technique is the method of choice to confirm the cyclization site by demonstrating a correlation between the two nuclei across the newly formed secondary amine. Indeed, a cross-peak between 5″-H_b and 2′-C observed for both **2a** and **2b** unambiguously cements the ring connectivity (Figure 3).[26]

^{15}N NMR Studies. To further cement the proposed structure and to evaluate the basicity of the new restricted antibiotics, ^{15}N NMR spectra of the TFA salts of compound **2a** and neomycin **1a** were recorded. Comparing the spectra at pH > 10.5 shows that while most amines exhibit similar chemical shifts, the ^{15}N signal of the 2′ amine in **2a** is approximately 5 ppm upfield shifted compared to the corresponding amine in the parent neomycin B **1a** (Figure 4). This observation further

(22) See Supporting Information for additional NMR spectra.

(23) Similar chemical shift changes have been predicted and observed for the corresponding carbon in cyclohexylammonium (51.6 ppm) vs *N*-methylcyclohexylammonium (59.4 ppm). See: Sarneski, J. E.; Surprenant, H. L.; Molen, F. K.; Reilley, C. N. *Anal. Chem.* **1975**, *47*, 2116−2124.

(24) This secondary carbon is clearly distinguished by its phase.

(25) This spectrum also unequivocally cements the assignment of the pseudosymmetrical 2-DOS ring.

(26) The cross-peak between 5″-H_a and 2′-C was not observed. As with H−H coupling, the value of this 3-bond coupling constant is dependent on the dihedral angle. The absence of cross-peaks is not uncommon and can be understood as the distortion of compounds **2a** and **2b** from a common conformation.

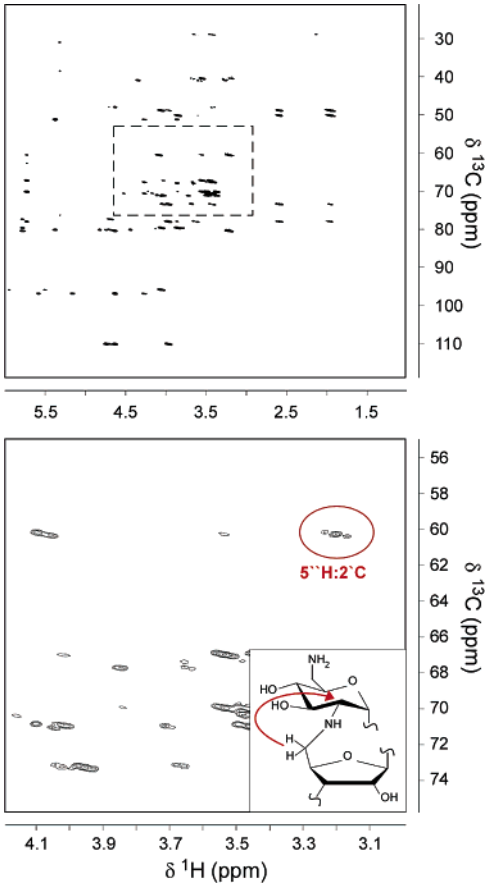

Figure 3. $^{1}H-^{13}C$ gHMBC spectrum of restricted neomycin B **2a** (top) and an expansion (bottom) highlighting the cross-peak from 5″-H_b to 2′-C.

supports the higher substitution of this particular nitrogen and is in agreement with the ^{13}C NMR and the reactivity data discussed above.

Recording the ^{15}N NMR spectra as a function of pH results in well-defined titration curves that can be fitted to yield the pK_a value of each amine (Figure 4 and Table 2).[27,28] The newly formed bridging secondary amine is found to have significantly attenuated basicity. With a pK_a value of 6.37, it is almost 2 pK_a units below the amine at the same position in neomycin B (pK_a 8.14). The lower basicity of this amine may be due to its crowded environment that hinders suitable solvation of the corresponding ammonium ion (and is in agreement with the low nucleophilicity exhibited by this functional group). Interestingly, the lower basicity of this center renders all other amines in **2a** more basic when compared to their corresponding amines in neomycin **1a** (Table 2), as would be expected based on intramolecular electrostatic considerations. For example, the pK_a of the NH_2 at position 1 of **2a** is 0.4 units higher than the analogous amine in neomycin **1a**. While these absolute pK_a values are likely to depend on the counterions,[29] the experimentally determined values clearly reflect the impact of cyclization on the basicity of the 2′-amine.

Ligand Binding to the A-Site RNA. Two recent contributions report the incorporation of the fluorescent nucleoside

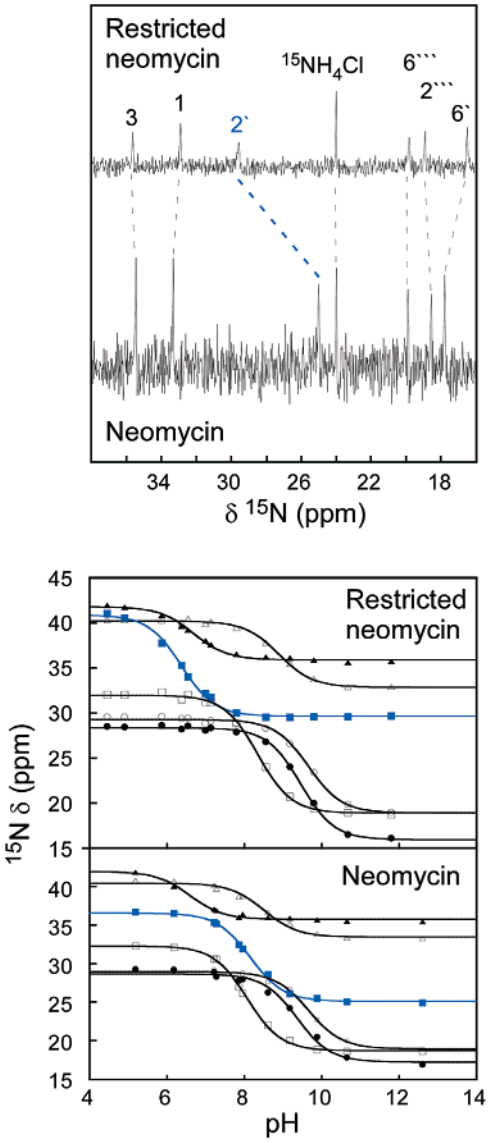

Figure 4. ^{15}N NMR spectra of restricted neomycin **2a** and neomycin **1a** at pH 10.7 show the distinct chemical shift of the 2′-nitrogen. The chemical shifts of each nitrogen are shown below as a function of pH. Symbols highlight individual nitrogens: 1 (open triangles), 2 (closed triangles), 2′ (blue filled squares), 6′ (filled circles), 2‴ (open squares), and 6‴ (open circles).

analogue 2-aminopurine (2AP) into the A-site as a means for detecting and quantifying aminoglycoside binding.[30] The 2AP substitution at A_{1492} accurately reports the unstacking of this nucleotide upon binding of the neomycin-class antibiotics. Notably, the magnitude of the 2AP fluorescence increase upon binding is relatively constant among different aminoglycosides and is strongly correlated with the specific structural changes that occur upon binding.[30] Capitalizing on these reports, the binding of the aminoglycosides discussed here was measured by titration into a fixed concentration (~200 nM) of A-site 2AP(1492) (Figure 5a,b). Using the directly measured 1:1 stoichiometry of paromomycin binding to the A-site, the fluores-

(27) Assignment of ^{15}N chemical shift is based on: Botto, R. E.; Coxon, B. J. *J. Am. Chem. Soc.* **1983**, *105*, 1021−1028.
(28) The pK_a values obtained for neomycin B are in good agreement with the values recently reported by Pilch. See: Kaul, M.; Barbieri, C. M.; Kerrigan, J. E.; Pilch, D. *J. Mol. Biol.* **2003**, *326*, 1373−1387.
(29) Kaul, M.; Barbieri, C. M.; Kerrigan, J. E.; Pilch, D. *J. Mol. Biol.* **2003**, *326*, 1373−1387.
(30) Kaul, M.; Barbieri, C. M.; Pilch, D. *J. Am. Chem. Soc.* **2004**, *126*, 3447−3453. Shandrick, S.; Zhao, Q.; Han, Q.; Ayida, B.; Takahashi, M., Takahashi; Winters, G. C.; Simonsen, K. B.; Vourloumis, D.; Hermann, T. *Angew. Chem., Int. Ed.* **2004**, *43*, 3177−3182.

Table 2. ^{15}N NMR Determination of pK_a Values for All Amine Groups

	neomycin (**1a**)			restricted neomycin (**2a**)		
amine	δ_{NH2} (ppm)[a]	δ_{NH3+} (ppm)[a]	pK_a[a]	δ_{NH2} (ppm)	δ_{NH3+} (ppm)	pK_a
1	33.5 ± 0.2	40.5 ± 0.2	8.50 ± 0.07	32.9 ± 0.1	40.2 ± 0.1	8.89 ± 0.04
3	35.8 ± 0.1	42.0 ± 0.3	6.59 ± 0.08	35.9 ± 0.1	41.8 ± 0.1	6.68 ± 0.04
2′	25.1 ± 0.1	36.6 ± 0.1	8.14 ± 0.03	29.7 ± 0.1	40.9 ± 0.2	6.37 ± 0.03
6′	17.2 ± 0.4	28.7 ± 0.2	9.36 ± 0.08	16.0 ± 0.1	28.4 ± 0.1	9.45 ± 0.03
2″′	18.7 ± 0.1	32.3 ± 0.1	8.07 ± 0.02	18.9 ± 0.1	32.0 ± 0.1	8.34 ± 0.03
6″′	18.9 ± 0.3	29.0 ± 0.2	9.65 ± 0.07	18.9 ± 0.2	29.3 ± 0.1	9.65 ± 0.04

[a] Tolerances indicate the standard error determined from curve fitting.

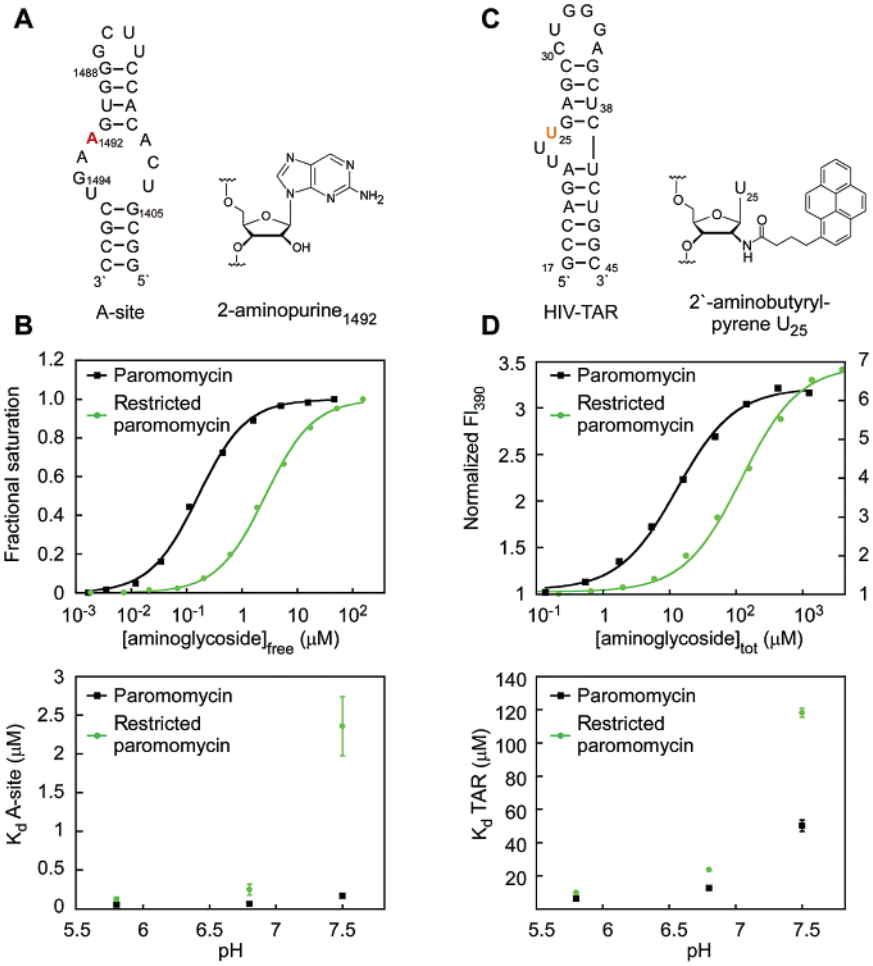

Figure 5. Measuring the RNA target binding of aminoglycosides. (A) Secondary structure of the fluorescently labeled A-site RNA used in this study, A-site 2AP (1492) RNA. Position 1492 is highlighted in red. The structure of 2-aminopurine is shown. (B) Sample binding isotherms of paromomycin (**1b**) and restricted paromomycin (**2b**) binding to A-site 2AP(1492) at pH 7.5. Shown below is the dependence of dissociation constants on pH. Error bars indicate plus or minus one standard deviation of three independent measurements. (C) Secondary structure of the fluorescently labeled TAR RNA used in this study, TAR 2′p(25) with position 25 highlighted in orange. The structure of the 2′-aminobutyrl-pyrene label is shown. (D) Sample binding isotherm of paromomycin (**1b**, right axis) and restricted paromomycin (**2b**, left axis) binding to TAR 2′p(25) at pH 7.5. The axes show the normalized increase in fluorescence upon aminoglycoside binding as described.[35] Shown in the bottom panel is the pH-dependence of binding. Error bars indicate plus or minus one standard deviation of three independent measurements.

cence increase upon binding of the aminoglycoside was converted to fractional saturation and plotted against the concentration of the unbound aminoglycoside. The binding isotherm fits well to a two-state binding model and yields a reproducible measure of binding affinity. Using this assay, paromomycin binds to the A-site at pH 7.5 with a K_d of 170 nM (Table 3), which compares favorably with literature reports.[31−33] Much like previous studies,[31,34] under the conditions used to measure paromomycin binding, neomycin binding to the A-site does not adhere to a simple two-state model and does not yield reproducible affinity values from this assay. Therefore, for the purpose of comparison, the approximate dissociation constant for the first neomycin binding event is compared here to the value of 19 nM at pH 7.5 measured by surface plasmon resonance.[31] Notably, restricted-neomycin **2a** does show single-state binding, much like paromomycin. This may implicate the 2′-amine as a contributor to neomycin's nonspecific binding.

(31) Alper, P. B.; Hendrix, M.; Sears, P. S.; Wong, C.-H. *J. Am. Chem. Soc.* **1998**, *120*, 1965−1978.
(32) Griffey, R. H.; Hofstadler, S. A.; Sannes-Lowery, K. A.; Ecker, D. J.; Crooke, S. T. *Proc. Natl. Acad. Sci. U.S.A.* **1999**, *96*, 10129−10133.
(33) Fourmy, D.; Recht, M. I.; Puglisi, J. D. *J. Mol. Biol.* **1998**, *277*, 347−362.
(34) Kaul, M.; Pilch, D. *Biochemistry* **2002**, *41*, 7695−7706.

Table 3. Target Binding Affinities of Aminoglycosides

	A-site		
	K_d[a] pH 5.8 (μM)	K_d pH 6.8 (μM)	K_d pH 7.5 (μM)
neomycin B **1a**	ND	ND	0.02[b]
restricted neomycin **2a**	0.07 ± 0.02	0.16 ± 0.01	0.42 ± 0.03
paromomycin **1b**	0.05 ± 0.02	0.06 ± 0.01	0.17 ± 0.01
restricted paromomycin **2b**	0.12 ± 0.03	0.35 ± 0.07	2.4 ± 0.4
	TAR		
	K_d pH 5.8 (μM)	K_d pH 6.8 (μM)	K_d pH 7.5 (μM)
neomycin B **1a**	1.2 ± 0.2	1.5 ± 0.2	2.4 ± 0.3
restricted neomycin **2a**	2.2 ± 0.6	3.8 ± 0.2	25.8 ± 0.6
paromomycin **1b**	6.2 ± 0.8	12.6 ± 0.4	50 ± 3
restricted paromomycin **2b**	9.6 ± 0.7	23.5 ± 0.2	118 ± 3

[a] Tolerances indicate the standard deviation of at least three independent determinations. [b] From Alper et al.[31]

At pH 7.5, the restricted-neomycin **2a** and restricted-paromomycin **2b** bind the A-site with 22- and 14-fold lower affinity, respectively, compared to neomycin and paromomycin, the parent natural products. This decreased binding affinity is likely to be largely due to the lower overall charge of the cyclized derivatives due to the diminished basicity of the 2′-amine in the restricted molecules. Indeed, upon decreasing the pH to 5.8 to more fully protonate this amine, the affinities of restricted-neomycin and restricted-paromomycin are only 3.8- and 2.3-fold lower than the parent aminoglycosides. Thus, under conditions where the overall protonation states are similar, the conformational restriction of these neomycin-class antibiotics only modestly decreases their binding affinity to the A-site.[36]

To correctly assess the effect of the conformational restraint on A-site binding, it is important that **1a** and **2a** bind at the same place on the A-site RNA. Previous dimethyl sulfate (DMS) footprinting studies indicate that aminoglycoside binding only modestly alters the A-site structure.[37,38] Specifically, the primary nucleotides whose reactivities significantly change in response to ligand binding are G_{1494}, G_{1405}, G_{1491}, and to a lesser extent G_{1497}. Using similar methods as those reported,[38] the DMS reactivity of a 3′-extended A-site RNA[39] indicates that binding of the restricted and nonrestricted paromomycin analogues reported here produce a similar footprint (Figure 6). As with previous studies, the primary ligand-dependent changes for both the nonrestricted and restricted aminoglycosides are at G_{1494}, A_{1493}, and G_{1497}, implying that the conformational constraint does not alter the structural context of the aminoglycoside interaction with the A-site. Furthermore, the magnitude of the ligand-dependent increase in 2-aminopurine fluorescence of

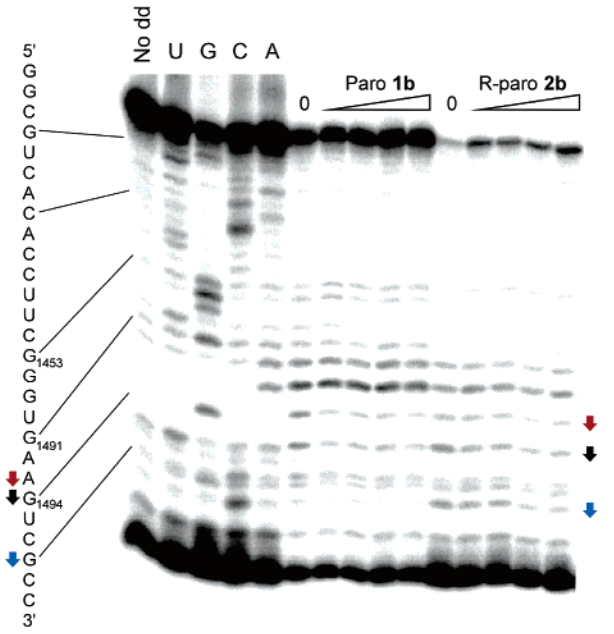

Figure 6. DMS modification footprint of aminoglycoside binding the A-site RNA, detected by primer extension. "No dd" lane shows the primer extension of untreated RNA without any dideoxy-NTPs present. U,G,C,A lanes are untreated RNA, sequenced using dideoxy-NTPs. "0" lanes show the modification by DMS and subsequent reduction and strand cleavage in the absence of aminoglycoside. DMS footprinting reactions in the presence of aminoglycoside are at concentrations corresponding to K_d, 4 × K_d, 16 × K_d, and 64 × K_d. The similarities in the footprint between aminoglycosides are noted as arrows, corresponding to a decrease in cleavage as the concentration of aminoglycoside is increased. Note that because aniline strand cleavage removes the modified nucleotide, primer extension stops indicated modification at one nucleotide closer to the 5′-end.

A-site 2AP(1492), which is strongly correlated with the structural changes at A_{1492} and A_{1493} that accompany binding,[30] is similar among all the aminoglycoside tested, also confirming that the structural details of the resulting complexes are similar.[40]

Ligand Binding to the HIV-1 TAR. Binding of all aminoglycosides to the TAR was measured using our previously validated and published assay, in which a 2′-aminobutyrylpyrene label at U_{25} accurately reports binding (Figure 5c,d).[35] At pH 7.5, restricted-neomycin **2a** and restricted-paromomycin **2b** bind the TAR with 11- and 2.4-fold lower affinity, respectively, when compared to neomycin and paromomycin (Table 3). Based on the structural design of these molecules, this modest decrease in affinity is surprising. More surprising, however, is that, upon decreasing the pH to 5.8 to more fully protonate the less basic secondary amine, the affinities of restricted-neomycin and restricted-paromomycin compared to the parent aminoglycosides are only 1.8- and 1.6-fold lower (Table 3). Thus, under conditions where the amine protonation states are normalized, restricting these neomycin-class antibiotics has no deleterious effect on binding to the HIV-1 TAR.

The surprising lack of deleterious effects of covalent cyclization on TAR binding prompted a deeper examination of the structural details of this RNA−ligand interaction. It is conceivable that the restricted aminoglycosides bind to different locations on the TAR or induce very different RNA structural changes upon binding. To examine this possibility, the RNase V1 footprint of each aminoglycoside on the TAR was evaluated as described.[35] RNase V1 cleaves primarily double-stranded or strongly stacked nucleotides. All natural and cyclized aminogly-

(35) Blount, K. F.; Tor, Y. *Nucleic Acids Res.* **2003**, *31*, 5490−5500.
(36) As the pH is decreased, the difference in affinity between neomycin and paromomycin decreases slightly. This suggests the possibility that the cause for convergence of the affinities of the restricted and nonrestricted aminoglycosides could include smaller, additional terms besides the pK_a of the 2′-amine.
(37) Miyaguchi, H.; Narita, H.; Sakamoto, K.; Yokoyama, S. *Nucleic Acids Res.* **1996**, *24*, 3700−3706.
(38) Recht, M. I.; Fourmy, D.; Blanchard, S. C.; Dahlquist, K. D.; Puglisi, J. D. *J. Mol. Biol.* **1996**, *262*, 421−436.
(39) The 3′ extended version of the A-site oligonucleotide, 5′-GGCGUCACACCUUCGGGUGAAGUCGCCGGUUGGCGUGGCUCGCG-3′, facilitates detection of DMS reactivity by primer extension via a 17-nucleotide DNA primer complimentary to the 3′-extension.

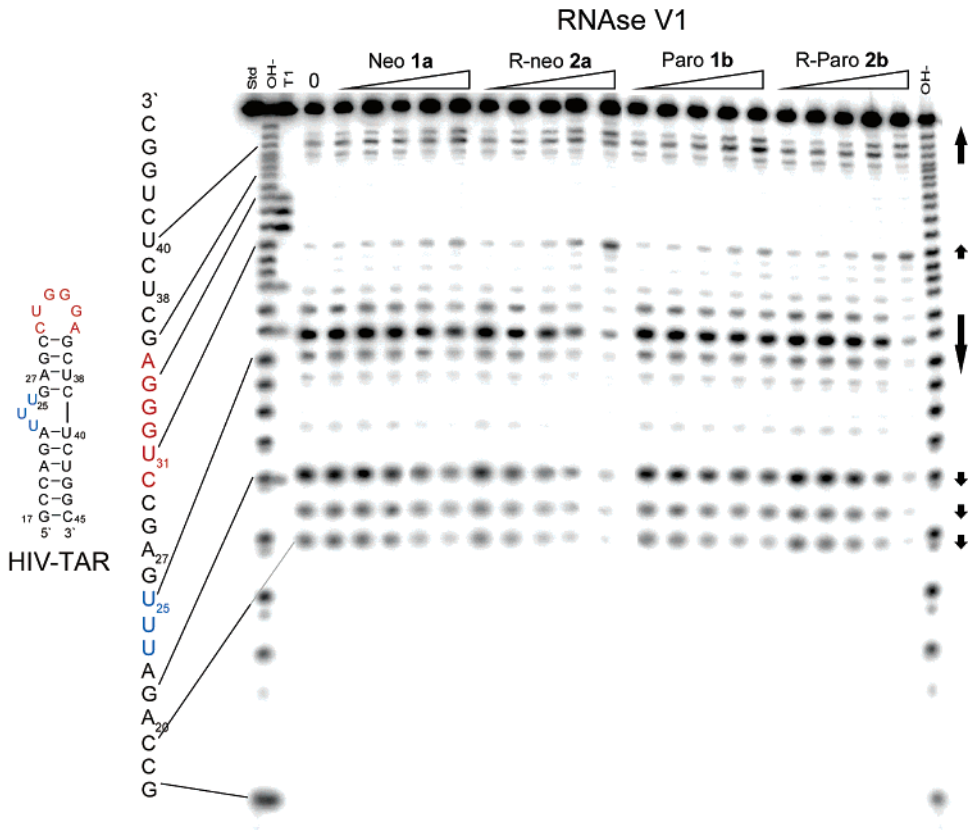

Figure 7. Enzymatic footprint (RNAse V1) of aminoglycoside binding to all 2′-hydroxy HIV-1 TAR. "Std" lanes are untreated RNA. "OH$^-$" lanes are an alkaline hydrolysis ladder of each RNA, and "T1" lanes show cleavage by ribonuclease T1 under denaturing conditions, in the absence of neomycin. "0" lane shows the cleavage by RNAse V1 in the absence of aminoglycoside. RNAse V1 footprints in the presence of aminoglycoside are at concentrations corresponding to 0.25 × K_d, K_d, 4 × K_d, 16 × K_d, and 64 × K_d. A strong cleavage indicates stacked or double-stranded regions of the structure. Similarities in the footprint between aminoglycosides are noted as arrows pointing up or down, corresponding to either increases or decreases in cleavage, respectively, as the concentration of aminoglycoside is increased. The loop and bulged regions are highlighted in the sequence as red or blue, respectively.

cosides tested herein generate a very similar RNase V1 footprint on the TAR (Figure 7). Most notable among these similarities are a ~2.5-fold increase in cleavage 3′ of C_{39} and U_{40} and at the 5′ side of the loop at U_{31}, and decreases in cleavage near the bulge at U_{25}, G_{26}, and A_{27}, and near the 5′-end at C_{19}, A_{20}, and G_{21}. Quantification of these changes as a function of aminoglycoside concentrations indicates a half-maximal protection concentration that agrees well with the data measured by the fluorescence assay (Supporting Information).[41] Thus, to the extent that RNAse V1 can detect, the location of the binding site and the TAR structural changes associated with binding are very similar among all the aminoglycosides tested here.

Discussion

Currently, numerous examples exist in the literature of low molecular weight ligands which bind to and alter the function of therapeutically important RNA targets.[8,9,42] Although much work has focused on ways to enhance the affinity of these interactions, comparatively little research has examined the issue of target selectivity.[16] Ultimately, for these molecules to be clinically successful, one will need to understand how to modulate their binding to a desired target, to the exclusion of competing targets within a cell. At present, the aminoglycosides are rather promiscuous binders, owing to both their electrostatic binding mode and their ability to conformationally adapt to diverse RNA folds. In an attempt to circumvent the latter, we have synthesized conformationally restricted aminoglycoside analogues designed to bind to the prokaryotic ribosomal A-site to the exclusion of the HIV-1 TAR. By measuring the binding of these novel aminoglycosides to both RNA targets, one can accurately assess and more thoroughly understand selectivity determinants.

A-Site−Restricted Aminoglycoside Interaction. As illustrated in Figure 1, the 2′-nitrogen and 5″-carbon of paromomycin are approximately 3.6 Å apart when bound to the A-site,[14] and a hydrogen bond is likely to exist between the proton of the 2′-nitrogen and the 5″-oxygen.[14] Thus, a newly formed 2′-N/5″-C covalent bond should constrain rings II and III in proximity and preorganize paromomycin into a conformation resembling the A-site bound form. In theory, this preorganization could be predicted to enhance the A-site binding affinity, due to a smaller change in the conformational entropy upon binding.[43] In practice, however, this phenomenon is seldom observed.[17] Rather, the decreased conformational entropy is often compensated for by enthalpic changes, resulting in similar

(40) Initial refinement of cocrystal diffraction data (T. Hermann, unpublished data) shows that **2a** binds within the A-site essentially the same as the parent **1a**. Thus, addition of the conformational restraint does not change the binding mode or grossly alter the ligand−RNA interaction.
(41) The half-maximal footprint of Ribonuclease A also corresponds well with the measured dissociation constants. See Supporting Information Figure S.19.
(42) Von Ahsen, U.; Davies, J.; Schroeder, R. *Nature* **1991**, *353*, 368−370.
(43) Estimates for loss of conformational entropy upon binding for one bond are ~0.6 kcal mol^{-1}. See: Nivotny, J.; Bruccoleri, R. E.; Saul, F. A. *Biochemistry* **1989**, *28*, 4735−4749.

affinities for constrained versus nonconstrained carbohydrates toward a specific target.[44] Alternatively, some minor structural adaptations, with an accompanying slight energetic cost, may still be necessary for **2b** to bind the A-site. Indeed, under conditions where their protonation states are equal, **1b** and **2b** bind the A-site with very similar affinities. Likewise, the neomycin derivatives **1a** and **2a** bind to the A-site with similar affinities.[40] Thus, despite not increasing the binding affinity, these conformational constraints can be tolerated isoenergetically, providing an opportunity for enhancement of selectivity among targets. This provides an important precedent for the rational design and development of conformationally restricted aminoglycosides.

TAR−Restricted Aminoglycoside Interaction. As illustrated in Figure 1, the 2′-nitrogen and 5″-carbon that are covalently linked in the restricted aminoglycosides **2a** and **2b** are ∼6.9 Å apart in neomycin when bound to the TAR. Since footprinting results indicate that the restricted aminoglycosides bind at the same site on the TAR as the parent compounds, it is surprising that both ligands are bound with comparable affinity to the nonrestricted parent compounds. This result is more baffling given the molecular dynamics prediction that the aminoglycoside conformation typically assumed while binding to the TAR is not easily accessed in solution by the restricted aminoglycosides. That is, the covalent link enforces an aminoglycoside "conformation" that is incompatible with the known structural data.

To qualitatively explore this apparent quandary, we used the PyMol structural viewing program to attempt to dock restricted neomycin onto the TAR. Specifically, a model aminoglycoside was created in which the neomycin glycosidic torsion angles resembled those encountered in the molecular dynamics simulation (Figure 2). In addition the conformation was altered so that rings II and III were close enough to form the 2′N/5″C bond. Since the neamine conformation is relatively constant among known aminoglycoside−RNA interactions, only modest changes were introduced in the torsional angles between rings I and II, and the position of ring I was not changed. The resultant model of **2a** (Figure 8) has torsional angles typically representative of the conformational space encountered in molecular dynamics simulations (Figure 2; Table 1) and is similar to the A-site bound structures. Furthermore, the $NH_3^+-NH_3^+$ distances within the aminoglycoside are consistent with the energetically favorable ranges reported for neomycin in solution.[45]

As Figure 8 clearly indicates, the interaction of the TAR with restricted neomycin must inherently be different than the neomycin interaction. As shown here, rings III and IV would encounter serious steric clash with the TAR backbone at A_{22} and U_{23} (yellow and green, respectively, in Figure 8) and the base of U_{23}. Two primary possibilities exist for how this could be overcome. The first is that the conformation and relative position of the neamine core could change more dramatically than expected, permitting a different orientation within the binding site with perhaps less steric clash. Energetically, this seems unlikely, given that the conformation of neamine is mostly conserved among known RNA−aminoglycoside interactions. Further, since the binding energy of aminoglycosides to the TAR

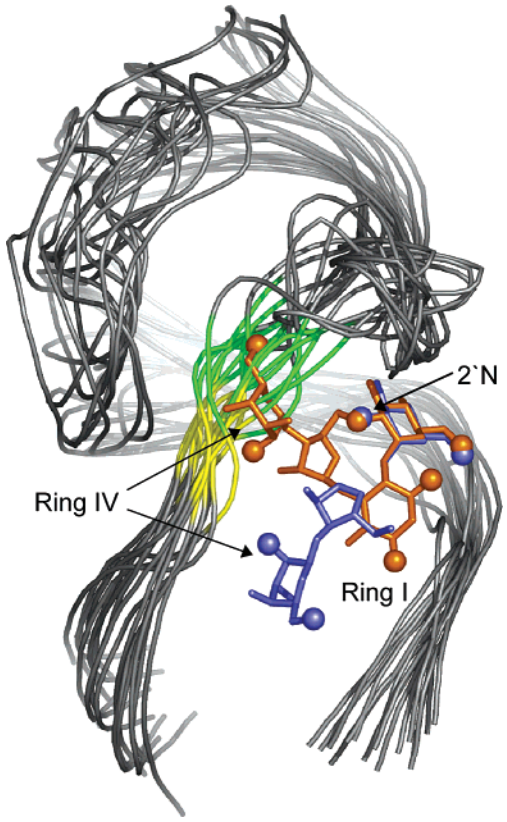

Figure 8. Structural implications of docking restricted neomycin **2a** (orange) onto the TAR. Grey traces represent the RNA backbone of the 17 best-fit NMR structures of the TAR with bound neomycin (blue). The backbone at U_{23} and A_{22} is highlighted in green and yellow, respectively. The torsional angles of this conformation of **2a** are $\Phi_{I/II} = 102.5$, $\Psi_{I/II} = -79.3$, $\Phi_{I,III} = -64.5$, $\Psi_{I/III} = 100.4$.

Table 4. Distance (Å) from Each Amine to the Nearest Phosphate When Bound to Different RNA Targets

	A-site	TAR
N1	6.4	3.1
N3	3.2	5.6
N2′	4.7	6.2
N6′	NA	7.1
N2‴	3.2	6.3
N6‴	4.8	6.8

is at least 30% electrostatic,[5,35] the position of the amines relative to RNA phosphate groups must be an important binding determinant. Of the six total amines on neomycin, N1 and N3 on ring I are the closest to neighboring RNA phosphate groups (Table 4), implying their energetic importance. If the binding energy provided by these amines is to be maintained, it seems unlikely that the relative position of this ring would be drastically altered.

The second possibility for overcoming the steric clash induced by the conformational restraint would be RNA structural adaptation. That is, the aminoglycoside binding site on the TAR may have the requisite plasticity to form significantly different structural interactions with the restricted or nonrestricted derivatives. From an RNA perspective, accommodation of the restricted neomycin conformer shown would require movement of U_{23} toward the major groove and a shift of the backbone at A_{22} by several angstroms. The ESR signature of a nitroxide label[46] at U_{23} demonstrates that it is very dynamic in the presence or absence of neomycin and, thus, could adapt without

(44) Carver, J. P. *Pure Appl. Chem.* **1993**, *65*, 763−770. Alibés, R.; Bundle, D. R. *J. Org. Chem.* **1998**, *63*, 6288−6301.
(45) Hermann, T.; Westhof, E. *J. Mol. Biol.* **1998**, *276*, 903−912.

serious energetic penalty.[47] The necessarily extensive movement of the backbone at A_{22} would further widen the minor groove and propagate other significant localized structural perturbations. Since this bulged region is largely single-stranded, the RNase V1 footprints can neither confirm nor deny these possible differences. However, quantification of the footprint at the 3′-side of the bulge at G_{26} suggests slight differences between the interaction with **2a** and **2b** or **1a** and **1b**.[48] Although it is unclear what energetic impact these possible RNA structural adaptations would have, it is clear that the structural interaction must be inherently different from the published TAR−neomycin structure. Thus, from either an aminoglycoside or an RNA perspective, it is apparent that, despite having a similar binding affinity, the restricted aminoglycosides must have a different structural binding interface with the TAR than the nonrestricted aminoglycosides.

TAR vs A-Site Specificity. The binding of aminoglycosides to RNA targets is highly promiscuous. The common paradigm is that this lack of selectivity is a consequence of the highly cationic nature of the aminoglycosides and the inherent flexibility of their glycosidic bonds. This "plasticity" facilitates a structural adaptation wherein the aminoglycosides can remodel themselves to match the electrostatic field generated by the RNA fold. In attempt to circumvent this promiscuous adaptation, we have introduced a conformational constraint into the aminoglycosides. Contrary to our design principles, the TAR RNA can bind these restricted aminoglycosides equally as well as the natural antibiotics. This suggests a converse paradigm; different RNA targets may exhibit varying degrees of selectivity for natural and modified aminoglycosides. Indeed, closer comparison of the interaction of aminoglycosides with either the A-site or TAR suggests that these therapeutically relevant RNA sites may possess inherently different selectivity traits. The aminoglycosides are more fully enveloped by the RNA fold of the A-site than in the TAR, as evidenced by solvent accessibility and the proximity of the amines to nearby phosphates (Table 4). Accordingly, thermodynamic data predict that four of five possible ion pairs are formed between paromomycin and the A-site,[34] whereas only two of six possible ion pairs are formed between neomycin and the TAR.[35] In addition, the very minimal chemical and enzymatic footprint of aminoglycoside binding to the A-site implies that it is a relatively preformed scaffold for aminoglycoside binding. In contrast, the footprinting data for aminoglycoside binding to the TAR indicate changes throughout the RNA, suggesting an inherently adaptable aminoglycoside binding scaffold. Finally, as demonstrated here, the TAR can accommodate a very different aminoglycoside structure with minimal deleterious effects on binding. Previous studies have suggested that the A-site is comparatively less forgiving of structural differences.[49] A notable example of the discriminatory difference of these two RNAs is the relative affinity to paromomycin and tobramycin. These two similarly charged aminoglycosides are bound by the TAR with roughly the same affinity.[35] In contrast, however, paromomycin binds the A-site with 10- to 20-fold higher affinity compared to tobramycin.[32,49] Thus the A-site is considerably more selective and less tolerant of the aminoglycoside structure compared to the TAR.

Summary

A straightforward synthesis affords two new and intriguing conformationally constrained aminoglycosides. Examining the affinity of these unique analogues to two different RNA targets, the A-site and the HIV-1 TAR, opens a window to the complex world of RNA selectivity. While we tend to view aminoglycosides as rather nonselective RNA binders, our results reveal that different RNA sites may exhibit inherently different ligand selectivity. The deeply encapsulating A-site appears to be a much more discriminating RNA target when compared to the "shallow" HIV TAR. For the future design of novel target selective therapeutics, it will be necessary to more fully consider the structural selectivity of the RNA target and not only the inherent selectivity displayed by the small molecules.

Experimental Section

Synthesis. All synthetic procedures and characterization as well as NMR spectra and assignment are included in the Supporting Information.

Materials. Neomycin and paromomycin were purchased as their sulfate salts from Sigma-Aldrich. Mes (4-morpholinoethanesulfonic acid), Mops (4-morpholinepropanesulfonic acid), and Hepes (4-(2-hydroxyethyl)-1-piperazineethanesulfonic acid) buffers, and all inorganic salts were purchased from Fisher (enzyme grade). Nonidet 40 was purchased from Fluka.

NMR Spectroscopy. ^{1}H, ^{13}C, and 2D NMR spectra were recorded on a Varian Mercury 400 MHz spectrometer. Dioxane was used as the internal standard ($\delta = 66.60$) for ^{13}C chemical shifts unless otherwise noted. ^{15}N NMR spectra were recorded at 50.7 MHz at 23 °C on a Varian Unity 500 spectrometer using a 5 mm inverse broad band probe with an acquisition time of 1 s and a recycle delay of 0.5 s. $^{15}NH_4Cl$ (1M, 10% enriched) in 85:15 (v:v) H_2O/D_2O contained in a coaxial 2-mm inner cell (from New Era) was used as an external reference ($\delta = 24.00$). The $^{15}NH_4Cl$ standard was purchased from Cambridge Isotope Laboratories, Inc. NMR solutions were prepared by dissolving aminoglycosides (TFA salt form, 340 mg each) in 0.5 mL 85:15 (v:v) H_2O/D_2O to yield the final concentration of 0.5−0.6 M. The solution pH was adjusted by 31% HCl and 40% KOH in 85:15 (v:v) H_2O/D_2O. All pH measurements were acquired with a Corning 320 pH meter interfaced with a microstem glass/calomel combination electrode (from Aldrich). The ^{15}N resonances were assigned according to Botto and Coxon.[27] The pK_a values were determined by fitting the data to the equation shown below using Kaleidagraph:

$$\delta = \frac{(\delta_{NH_2} - \delta_{NH_3})(10^{pH-pK_a})}{1 + 10^{pH-pK_a}} + \delta_{NH_3}$$

Molecular Dynamics Simulations. For both neomycin and restricted neomycin, simulations in a box of explicit water (∼580 H_2O and 4 Cl^-) were run under periodic boundary conditions at a time step of 1 fs. AMBER[50] force field parameters were used as described in our previous aminoglycoside simulations.[45] 100 cycles each of heating to 5000 K for 10 ps followed by cooling to 10 K over 5 ps were performed. Structures were extracted at the end of the 10 K cycles and subjected to 1000 steps of conjugate gradient minimization. Torsion angles were measured and recorded. There was no filtering for high-energy structures

(46) Edwards, T. E.; Sigurdsson, S. T. *Biochemistry* **2002**, *41*, 14843−14847.
(47) The NMR solution structure also reveals significant mobility for this residue. See ref 12.
(48) Quantification of RNAse V1 footprint indicates that **2a** and **2b** may induce more protection at G_{26} than **1a** and **1b**.
(49) Simonsen, K. B.; Ayida, B.; Vourloumis, D.; Takahashi, M.; Winters, G. C.; Barluenga, S.; Qamar, S.; Shandrick, S.; Zhao, M.; Hermann, T. *ChemBioChem* **2002**, *3*, 1223−1228.
(50) Cornell, W. D.; Cieplak, P.; Bayly, C. I.; Gould, I. R.; Merz, K. M. J.; Ferguson, D. M.; Spellmeyer, D. C.; Fox, T.; Caldwell, J. W.; Kollman, P. A. *J. Am. Chem. Soc.* **1995**, *117*, 5179−5197.

which might be conformationally trapped by the solvent or ions. However, comparison of plots without the 50% highest energy conformations showed no significant difference in distribution of the conformers over the map.

Preparation of Oligonucleotides. All oligonucleotides were purchased from Dharmacon RNA technologies (Lafayette, CO), deprotected as per manufacturer protocol, and lyophilized. The deprotected oligonucleotides were resuspended in water and purified using 20% denaturing PAGE. Excised gel slices were eluted overnight into a buffer containing 50 mM Hepes pH 7.5 and 1 M NaCl, followed by ethanol precipitation. After a 70% ethanol/water wash, the RNA pellets were dried and resuspended in water, quantified by UV absorbance, and their identities were confirmed by MALDI-TOF mass spectrometry. For binding experiments, the TAR was refolded by heating a 15 μM solution of the pyrene-labeled TAR in a Tris binding buffer (50 mM Tris pH 7.4, 100 mM NaCl, 1 mM $MgCl_2$) to 95 °C for 5 min, followed by cooling on ice for 20 min. Correspondingly, the A-site RNA was refolded by heating a 15 μM solution of A-site 2AP(1492) in the A-site binding buffer (20 mM Hepes 7.5, 100 mM NaCl, 0.5 mM EDTA) to 65 °C for 5 min, followed by cooling at room temperature for 20 min.

Fluorescence Binding Assays. All fluorescence spectra were measured on a Perkin-Elmer LS50B fluorimeter, with an excitation slit width of 10 nm and an emission slit width of 10 nm. Upon excitation at 345 or 310 nm for TAR 2′p(25) or A-site 2AP(1492), respectively, the emission spectrum was recorded three times (scan rate of 400 nm/min) and averaged for a composite spectrum. As we have previously observed, ideal solution conditions for measuring binding to TAR 2′p(25) include 100 mM NaCl and 1 mM $MgCl_2$. Optimal solution conditions for measuring binding to A-site 2AP(1492) include 100 mM NaCl and 0.5 mM EDTA, consistent with literature reports.[29,30] To buffer the pH, the titrations were performed in the sulfonate buffers Mes, Mops, or Hepes for pH values of 5.8, 6.8, or 7.5, respectively. The amount of NaOH added to each to adjust to the appropriate pH was recorded and found to give less than 5 mM difference in total sodium ion concentration over the this pH range. Notably, at low pH values the fluorescence of TAR 2′p(25) quenched dramatically upon saturation with each aminoglycoside. Inclusion of 0.001% nonionic detergent P40 (Fluka) in all TAR titrations alleviated this problem, suggesting aggregative behavior in the presence of fully protonated aminoglycosides.

For a typical binding experiment, the fluorescence spectrum of a 148 μL solution of buffer in the absence of any RNA or aminoglycoside was recorded. This spectral blank, for which only Raman scatter was observed, was subtracted from all subsequent spectra within each binding experiment. Following determination of the buffer blank, 2 μL of a 15 μM solution of refolded RNA was added (final concentration is 200 nM), the solution was mixed, and the spectrum was again recorded. Subsequent aliquots of 1 μL of an aqueous aminoglycoside solution (increasing concentrations) were added, and the fluorescence spectrum was recorded after each aliquot until the fluorescence signal saturated. Over the entire range of aminoglycoside concentrations, the emission maxima of both fluorophores varied less than 1.5 nm. To correct for the presence of any fluorescent contamination in each aminoglycoside, the full titration was repeated in the absence of labeled RNA. Any observed "background" at the emission maximum was then subtracted from each corresponding point of the labeled RNA titrations, and the resulting fluorescence intensity was corrected for dilution.

Based on definitive literature reports and direct measurements, a two-state model for a 1:1 interaction was assumed for the A-site, and the corrected fluorescence at each titration point, Fl_i, was converted to a fractional fluorescence saturation (f_{sat}):

$$f_{sat} = \frac{(Fl_i - Fl_0)}{(Fl_\infty - Fl_0)}$$

where Fl_0 and Fl_∞ are the observed fluorescence in the absence of aminoglycoside, or at saturation, respectively. As previously described,[51] the concentration of free aminoglycoside, $[ag]_{free}$, can be calculated from this fractional saturation and the total aminoglycoside concentration, $[ag]_{tot}$:

$$[ag]_{free} = [ag]_{total} - f_{sat}*[RNA]_{tot}$$

The subsequent plot of f_{sat} against $[ag]_{free}$ was fit to the equation for a simple binding isotherm:

$$f_{sat} = \frac{([ag]_{free}/K_d)}{(1 - [ag]_{free}/K_d)}$$

For the TAR, the corrected fluorescence intensity value at each titration point (Fl_i) was then normalized to the initial fluorescence of the pyrene-derivatized TAR in the absence of aminoglycoside (Fl_0) and plotted as a function of the dilution-corrected aminoglycoside concentration as shown in Figure 2. From this plot, an accurate binding affinity and Hill coefficients for the interaction of each aminoglycoside with the TAR were determined as described.[35]

DMS Footprint of Aminoglycosides on the A-Site. DMS footprinting experiments were performed essentially as described.[38] Briefly, 2 μL of a 1:2 dilution of DMS in ethanol was added to a 75 nM solution of an 3′-extended A-site RNA (includes additional 3′-end nucleotides: 5′-GGUUGGCGUGGCUCGCG-3′) in a total volume of 50 μL of a buffer containing 80 mM sodium cacodylate pH 7.5, 50 mM NaCl, 0.4 mM EDTA, and the indicated concentration of aminoglycoside. After 30 min at room temperature, the reaction was stopped by addition of 12.5 μL of DMS stop buffer, resulting in the final additional concentrations of 150 mM Tris pH 7.5 and 200 mM β-mercapto-ethanol. Each reaction was then precipitated with the addition of 30 μg of Glycoblue (Ambion, Austin, TX), 12 μL of 3 M NaOAc, and 320 μL of ethanol. Sodium borohydride reduction and subsequent aniline cleavage were performed as described,[38] except that 30 μg of Glycoblue was added to aid quantitative precipitation at each step.

After resuspending in water, ~250 fmol of each RNA was combined with ~125 fmol of a 5′-[^{32}P]-labeled DNA primer (5′-CGCGAGCCACGCCAACC-3′) in a buffer of 50 mM Tris pH 8.3, 60 mM NaCl, and 10 mM DTT. This mixture was heated to 95 °C for 5 min, followed by immediately cooling on dry ice/ethanol for 1 min. After briefly centrifuging, $Mg(OAc)_2$ in the same buffer was added to a final concentration of 6 mM. While maintaining the same buffer conditions, deoxy NTPs (625 μM final concentration, Promega) and 1 unit of AMV-reverse transcriptase (Invitrogen) were added to the RNA/primer mix, and the solution was incubated at 42 °C for 30 min. These reactions were quenched by dilution into an equal volume of loading dye (88% formamide with 0.02% bromophenol blue and xylene cyanol), followed by immediate separation with 20% denaturing PAGE. To aid interpretation, sequencing reactions containing one dideoxyNTP were performed as per manufacturer protocol.

RNase Footprint of Aminoglycosides on the TAR. A trace concentration (<20 pM) 5′-[^{32}P]-labeled, refolded TAR (95 °C 5 min, ice 20 min) was incubated with 1.6 milliunits of ribonuclease V1 (Ambion) for 15 min at room temperature in a solution containing 30 mM Tris pH 7.5, 100 mM NaCl, 2 mM $MgCl_2$, 0.1 μg/mL yeast torula RNA (Ambion), and the indicated concentrations of aminoglycosides (Figure 6). These reactions were quenched by dilution into an equal volume of loading dye (88% formamide with 0.02% bromophenol blue and xylene cyanol), followed by immediate separation with 20% denaturing PAGE.

Ribonuclease T1 reactions contained a trace concentration (<20 pM) of 5′-[^{32}P]-labeled, refolded TAR and 1 unit of ribonuclease T1 (Boerrhinger Moenheim) in a solution of 20 mM sodium citrate pH 5.0, 1 mM EDTA, 3.63 M urea, and 0.05 μg/μl yeast torula RNA

(51) Winzor, D. J.; Sawyer, W. H. *Quantitative Characterization of Ligand Binding*; Wiley-Liss, Inc.: New York, 1995.

(Ambion). These reactions were incubated at 55 °C for 20 min, followed by dilution into an equal volume of loading dye and separation with 20% denaturing PAGE.

Alkaline Hydrolysis Reactions. A trace amount (<20 pM) of 5′-[^{32}P]-labeled TAR was incubated in a buffer of 50 mM $NaHCO_3$ pH 9.0 at 95 °C for 7 min, followed by quenching on ice for 10 min. After dilution with an equal volume of loading dye, the reactions were separated on 20% PAGE. All polyacrylamide gels were run for approximately 3 h at 20 W and analyzed using a Molecular Dynamics Storm Phosphorimager.

Acknowledgment. Dedicated to Professor Peter B. Dervan on the occasion of his 60th birthday. We are grateful to Drs. Qiang Cong and John Wright for their help with the NMR experiments. Special thanks to DeLano Scientific (San Carlos, CA) for use of the open-source PyMol molecular graphics system. This work was generously supported by the National Institutes of Health (Grant Number AI 47673 to Y.T., GM 065652 to K.B. and AI51104 to T.H.).

Supporting Information Available: Synthesis procedures, characterization as well as 1D and 2D NMR spectra of key intermediates and final compounds. This material is available free of charge via the Internet at http://pubs.acs.org.

JA050918W